

pubs.acs.org/biochemistry Article

Negative Cooperativity in the Mechanism of Prenylated-Flavin-Dependent Ferulic Acid Decarboxylase: A Proposal for a "Two-Stroke" Decarboxylation Cycle

April K. Kaneshiro, Prathamesh M. Datar, and E. Neil G. Marsh*



Cite This: https://doi.org/10.1021/acs.biochem.2c00460



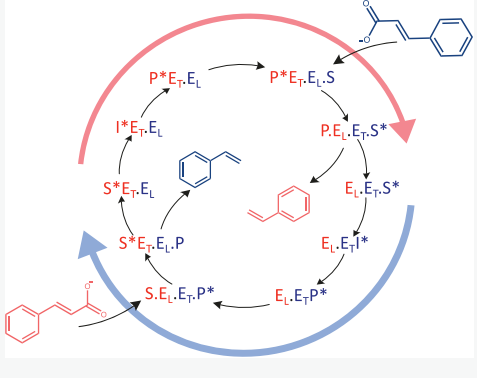
ACCESS

Metrics & More

Article Recommendations

Supporting Information

ABSTRACT: Ferulic acid decarboxylase (FDC) catalyzes the reversible carboxylation of various substituted phenylacrylic acids to produce the correspondingly substituted styrenes and CO_2 . FDC is a member of the UbiD family of enzymes that use prenylated-FMN (prFMN) to catalyze decarboxylation reactions on aromatic rings and C–C double bonds. Although a growing number of prFMN-dependent enzymes have been identified, the mechanism of the reaction remains poorly understood. Here, we present a detailed pre-steady-state kinetic analysis of the FDC-catalyzed reaction of prFMN with both styrene and phenylacrylic acid. Based on the pattern of reactivity observed, we propose a "two-stroke" kinetic model in which negative cooperativity between the two subunits of the FDC homodimer plays an important and previously unrecognized role in catalysis. In this model, catalysis is initiated at the high-affinity active site, which reacts with phenylacrylate to yield, after decarboxylation, the covalently bound styrene—prFMN cycloadduct.



In the second stage of the catalytic cycle, binding of the second substrate molecule to the low-affinity active site drives a conformational switch that interconverts the high-affinity and low-affinity active sites. This switching of affinity couples the energetically unfavorable cycloelimination of styrene from the first site with the energetically favorable cycloaddition and decarboxylation of phenylacrylate at the second site. We note as a caveat that, at this point, the complexity of the FDC kinetics leaves open other mechanistic interpretations and that further experiments will be needed to more firmly establish or refute our proposal.

INTRODUCTION

Enzyme-catalyzed decarboxylation reactions are ubiquitous in both primary and secondary metabolism; however, decarboxylation reactions often proceed through highly unfavorable transition states associated with the accumulation of negative charge on the α -carbon. Therefore, nature has evolved a remarkably diverse range of cofactors that can function as electron sinks in decarboxylation reactions; well-studied examples include pyridoxal phosphate and thiamine pyrophosphate and Lewis acidic metal ions. Decarboxylases have also attracted considerable interest for their ability to function as "green" catalysts capable of catalyzing both decarboxylation and C–C bond-forming reactions under mild conditions. 6,7

The most recently discovered decarboxylation cofactor is prenylated-FMN (prFMN). This cofactor appears to be widespread in microbes and is used to facilitate decarboxylation reactions at sp²-hybridized carbon atoms in double bonds and aromatic rings that otherwise would be unreactive. In prFMN, the isoalloxazine ring system of the flavin is modified by the addition of a fourth ring that bridges the flavin C6 and N5 positions and is derived from an isoprene unit. This modification is performed by a specialized prenyl transferase that uses reduced FMN and either dimethylallyl phosphate (in bacteria 15) or dimethylallyl

pyrophosphate (in yeast¹⁶) as substrates.¹⁷ prFMN-dependent decarboxylases are often referred to as UbiD-like decarboxylases after UbiD, the enzyme that catalyzes the decarboxylation of 4-hydroxy-3-octaprenylbenzoic acid to 2-octaprenylphenol as part of ubiquinone biosynthesis in many bacteria.^{18–20}

Ferulic acid decarboxylase (FDC)^{11,12,21} was the first enzyme to be structurally characterized, leading to the identification of prFMN, and remains the best understood. The decarboxylation mechanism involves an unusual 1,3-dipolar cycloaddition between the substrate and prFMN, as shown in Figure 1 for the decarboxylation of phenylacrylic acid.^{11,21} The crystal structures²² of the enzyme reacted with either substrates or substrate analogues that form covalent adducts with prFMN support the formation of several of the intermediates shown in Figure 1. Complementary evidence comes from high-resolution native mass spectrometry experi-

Received: August 10, 2022 Revised: November 15, 2022



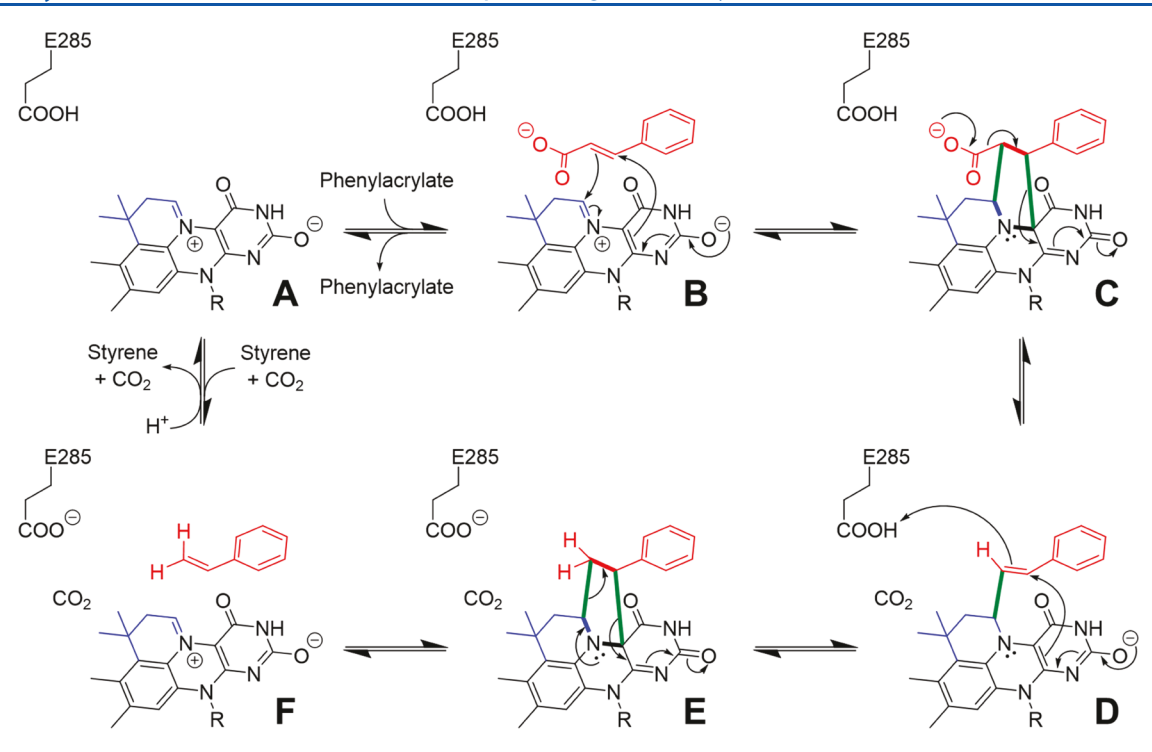


Figure 1. Proposed 1,3-dipolar cycloaddition mechanism of FDC. The iminium species of prFMN (species A) undergoes a 1,3-dipolar cycloaddition with phenylacrylate (intermediate B), resulting in a cycloadduct (intermediate C). Next, decarboxylation is coupled to the cleavage of the C4a-C β bond, forming a single-tethered adduct (intermediate D). A proton is transferred from a conserved active site glutamic acid resulting in the styrene cycloadduct (intermediate E). Finally, a cycloelimination releases the product, styrene, and reforms the iminium form of prFMN (species F).

ments that allowed the cycloadducts of prFMN with the product, styrene, and with a mechanism-based inhibitor mimicking the structure of the substrate, phenylacrylate, to be identified. Computational studies that model the energetics of forming cycloadducts between prFMN and phenylacrylic acid further support the feasibility of the mechanism. 4

In contrast to the identity of the chemical intermediates in the FDC mechanism, which are supported by various lines of experiment, the kinetics of the FDC-catalyzed reaction has not been extensively investigated. Previously, we reported presteady-state kinetic analyses of FDC from S. cerevisiae reacting with phenylacrylic acid that uncovered complex kinetic behavior that most likely arises from negative cooperativity between the two active sites of the enzyme dimer.²³ Here, we extend our kinetic analysis of FDC using stopped-flow UVvisible spectroscopy to examine the reaction of the enzyme with both styrene and phenylacrylate at concentrations ranging from sub-stoichiometric to several-fold molar excess. Based on our experiments, we propose a "two-stroke" mechanism for the FDC-catalyzed reaction in which conformational changes transmitted between the two subunits drive the release of styrene from the active site to complete the catalytic cycle.

MATERIALS AND METHODS

Reagents. Trans-phenylacrylic acid, d_7 -trans-phenylacrylic acid, styrene, and d_8 -styrene were all purchased from Sigma-Aldrich Co. All other materials were purchased from Sigma-Aldrich Co. or Thermo Fisher Scientific Co.

Expression and Purification of FDC. Expression and purification of recombinant *S. cerevisiae* holo-FDC from *Escherichia coli* were performed as described previously.¹⁰

The cofactor content of the purified holo-enzyme evaluated by UV—visible spectroscopy and LC-MS and found not to vary significantly from batch to batch. The UV—visible and mass spectra of a typical batch of holo-enzyme are shown in Figure S1 of the Supporting Information.

Stopped-Flow Absorption Spectroscopy. Experiments were performed essentially as described previously²³ using a Hi-Tech Scientific SF-61 DX2 double-mixing instrument (TGK Scientific) controlled by Kinetic Studios software package (TGK Scientific). Time-dependent absorption spectra were recorded using a charged-coupled device, whereas single wavelength measurements were recorded using a monochromator coupled with a photomultiplier tube. Experiments were performed at 4 °C, with both enzyme and substrate solutions prepared in 50 mM potassium phosphate, 10% (v/v) glycerol, pH 7.5. FDC was made anaerobic by introducing the solution into a glass tonometer and between evacuation and flushing with argon gas. Phenylacrylate solutions were transferred to glass syringes and made anaerobic by bubbling argon gas through for 10 min before use. Due to its volatility, styrene was added directly to a syringe of anaerobic buffer and used immediately to minimize the introduction of oxygen.

Data Averaging. Stopped-flow data were typically recorded under identical experimental conditions at different timescales to obtain data with high temporal resolution on the millisecond to second timescale. Generally, three to five stopped-flow shots were averaged to improve the signal-tonoise ratio before fitting. This process was repeated for a variety of time ranges to improve the quality of data at all times of interest. The time dimension was binned using 100 bins for each order of magnitude and absorbance values averaged as described previously.²³

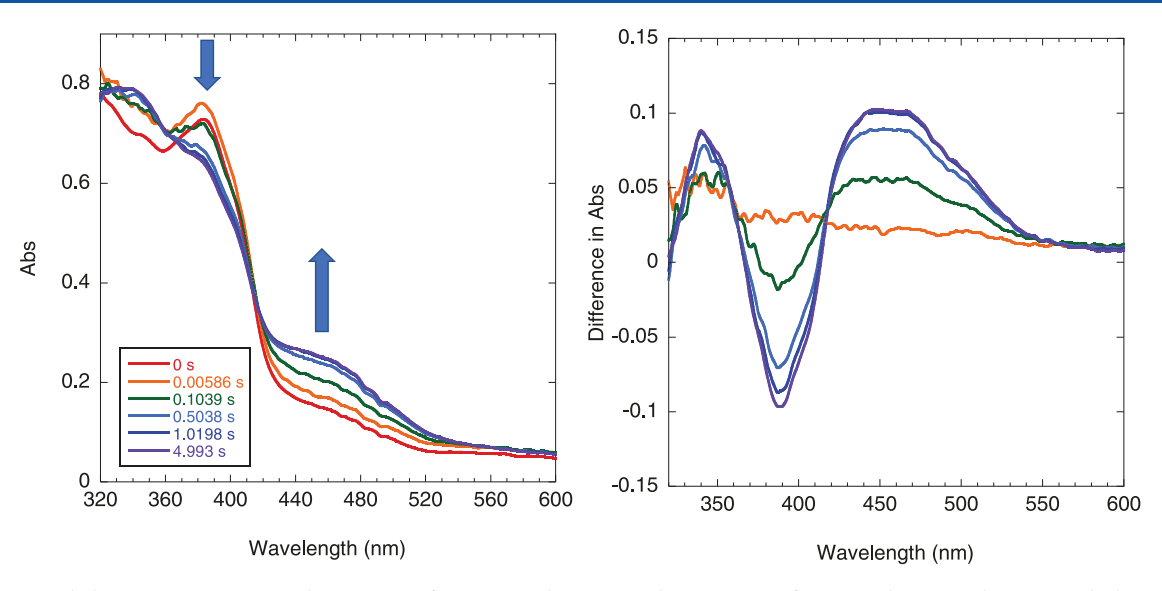


Figure 2. Spectral changes accompanying the reaction of prFMN with styrene. The spectrum of unreacted FDC is shown in red; the spectrum of the styrene adduct is shown in blue.

RESULTS

Reaction of FDC with Styrene. In the absence of CO₂, styrene can only react to form the prFMN cycloadduct. Therefore, we reasoned that the kinetics for this reaction should be more straightforward to interpret than for the enzyme reacting with phenylacrylate. The UV-visible spectral changes associated with the reaction of 180 µM holo-FDC with 1 mM styrene (final concentrations after mixing) are shown in Figure 2. Most noticeably, there is an increase in absorbance of the broad feature centered around 460 nm and a decrease in the sharper band centered at 380 nm. Under the conditions of the experiment, the spectral changes were essentially complete after 5 s, and the final spectrum of the styrene-reacted enzyme is essentially identical to that obtained previously when the enzyme was reacted with phenylacrylic acid.²³ This observation is consistent with our previous studies that show the prFMN-styrene cycloadduct is the species that accumulates on the enzyme at equilibrium.²³

Pre-steady-State Kinetics of Styrene Reaction. We used UV-visible stopped-flow spectroscopy to investigate the kinetics of styrene reacting with FDC. In particular, we aimed to investigate whether negative cooperativity between the two active sites of the FDC dimer (suggested by the previous experiments²³) plays a role in the reaction. Therefore, we varied the styrene concentration from 1 mM to 60 μ M while keeping the FDC concentration fixed at 180 μ M (concentrations after mixing, reaction at 4 °C). The highest concentration represents a ~5-fold molar excess of the substrate over enzyme, whereas the lowest concentration is sub-stoichiometric with enzyme so that on average only one active site in the FDC dimer should have substrate bound.

Based on our previous studies, ²³ the kinetics of the reaction were monitored at the following wavelengths: 380 nm, which monitors the consumption of prFMN; 460 nm, which monitors the formation of the styrene–prFMN cycloadduct; and 425 nm, which also monitors the formation of a styrene–prFMN cycloadduct but which is characterized by a spectrum blue-shifted by ~35 nm that has a smaller extinction coefficient. ²³ As discussed later, the blue-shifted and redshifted cycloadducts likely represent the same chemical species,

but they experience different active site environments. (We note that at all wavelengths, there was a very rapid initial decrease in absorbance that was nearly complete within the mixing time of the spectrometer. This appears to be a mixing artifact as it was present when the enzyme was shot against plain buffer. Therefore, the first 3 ms of each reaction were excluded from the kinetic analysis.)

The kinetics of styrene reacting with FDC is unexpectedly complicated. Three kinetic phases are observed at each wavelength and at each styrene concentration (Figure 3). The absorbance changes observed at 380 and 460 nm closely mirror each other (Figure 3A,B), which is consistent with the conversion of the prFMN:styrene Michaelis complex (absorbance maximum 380 nm) to the prFMN-styrene cycloadduct (absorbance maximum 460 nm). In contrast, when the reaction was monitored at 425 nm, a somewhat different kinetic profile was observed. At the lower styrene concentrations, 60 and 90 µM, the absorbance initially increases and then declines, consistent with the formation of an intermediate. However, at higher substrate concentrations, the absorbance continues to increase at longer times. This increase partially masks the decrease in absorbance seen at low concentrations, which is still evident at this wavelength even at high styrene concentrations. For the fastest phase, both the rate and amplitude appear fairly independent of styrene concentration. The next phase, however, is clearly concentration-dependent as its amplitude continues to increase with increasing styrene concentration, although the rate changes little. The slowest phase appears, again, to be concentration-independent in both rate and amplitude.

The data were globally fitted using the program GraphPad Prism (see the Supporting Information for details). The data could be robustly fitted by three apparent first-order rate constants, $k_{1\text{sty}}$, $k_{2\text{sty}}$, and $k_{3\text{sty}}$, shared across the entire data set, with the amplitudes associated with each rate constant allowed to vary. The values obtained for the rate constants are $k_{1\text{sty}} = 45 (44-48) \text{ s}^{-1}$, $k_{2\text{sty}} = 8.2 (7.7-8.8) \text{ s}^{-1}$, and $k_{3\text{sty}} = 2.7 (2.6-2.8) \text{ s}^{-1}$ (95% confidence intervals in parentheses). The individual amplitudes associated with each rate constant varied somewhat as a function of styrene concentration, most of which we attribute to signal noise as the absorbance changes

Biochemistry pubs.acs.org/biochemistry Article

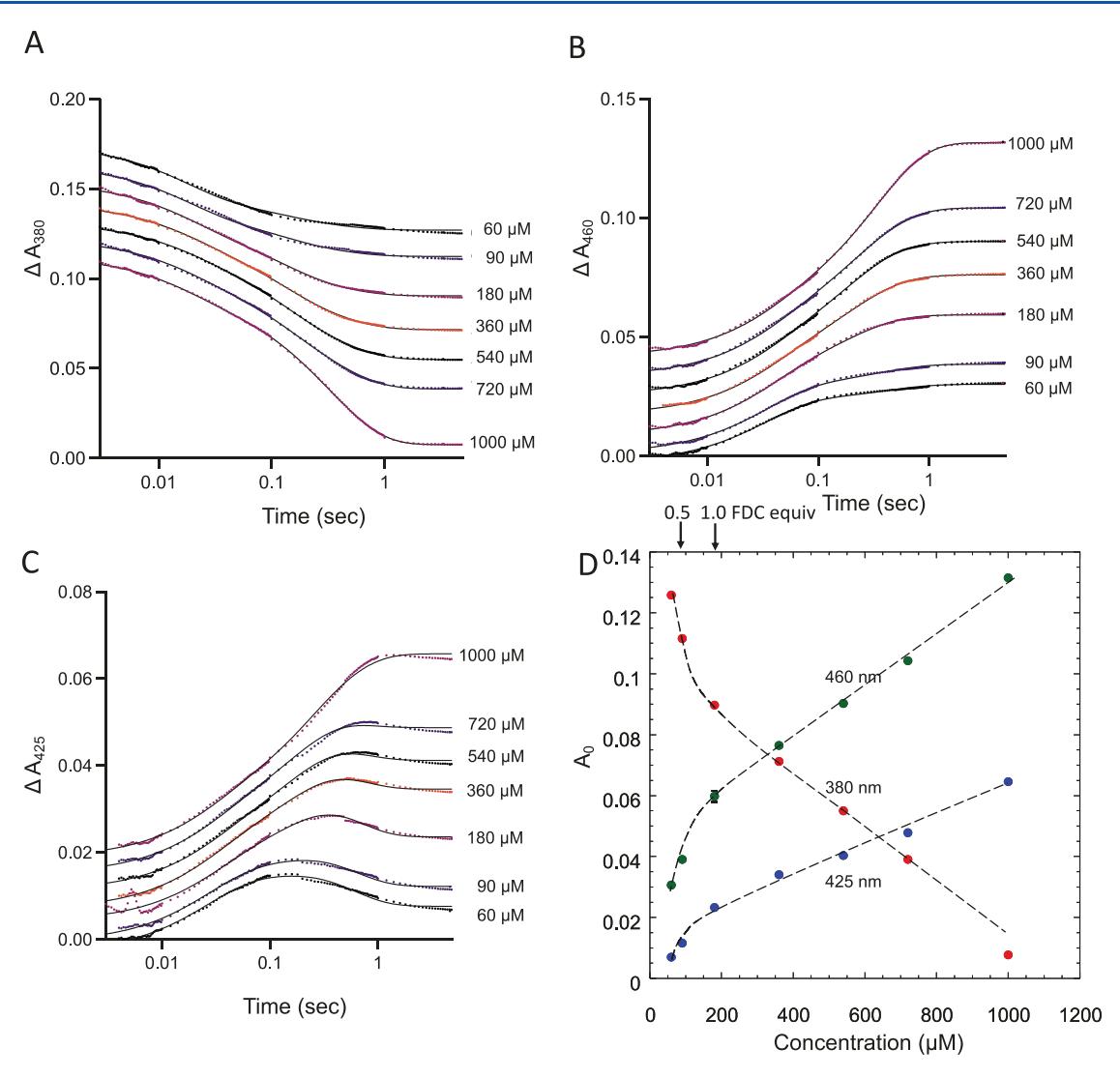


Figure 3. Pre-steady-state kinetics of FDC reacting with styrene. FDC was reacted with increasing concentrations of styrene as indicated, and the reaction was monitored at (A) 380 nm, (B) 460 nm, and (C) 425 nm. *Note:* the absorbance traces have been offset for clarity. The data were globally fitted to a three-exponential function as described in the text. **D:** The total changes in absorbance (recorded after 5 s) at the different wavelengths are plotted as a function of styrene concentration for each wavelength monitored. The dashed lines are interpolated between the data points. The concentrations of styrene corresponding to 0.5 and 1.0 FDC active sites are marked above the plot.

are quite small. However, the sum of the amplitudes ($A_{\text{tot}} = A_{1\text{sty}} + A_{2\text{sty}} + A_{3\text{sty}}$) exhibits a clear trend in which the signal initially increases sharply as a function of styrene concentration and then increases more gradually (Figure 3D). The inflection point in the curve occurs at a substrate to enzyme ratio of ~ 0.5 and, interestingly, even at the highest styrene concentration, shows no evidence of saturation.

Reaction of FDC with Phenylacrylic Acid. We have previously investigated the pre-steady-state kinetics of FDC reacting with phenylacrylic acid, ²³ however, informed by the results obtained with styrene, we extended our studies to cover a wider range of substrate concentrations and, in particular, to examine the reaction at sub-stoichiometric concentrations. Accordingly, holo-FDC, 180 μ M after mixing, was reacted at 4 °C with final concentrations of phenylacrylate ranging from 1 mM to 45 μ M, and the reaction was monitored at 380, 425, and 460 nm over the course of 5 s, as shown in Figure 4.

The absorbance changes observed with phenylacrylate as the substrate (Figure 4) are similar to those seen with styrene, reflecting the fact that similar adducts are formed with prFMN

by both molecules. However, in this case, the kinetic behavior is more complex. The added complexity most likely arises because the initially formed phenylacrylate-prFMN cycloadduct then undergoes decarboxylation to form the styreneprFMN adduct, which previous studies have shown is the species that accumulates on the enzyme. Although it is hard to discern from the traces monitored at 380 and 460 nm, it is clearly evident from the traces obtained at 425 nm that the reaction exhibits four phases, the amplitudes of which are dependent on phenylacrylate concentration. Most noticeably, the slower two phases have amplitudes that are markedly concentration-dependent, and at the lowest phenylacrylate concentrations, 45 and 90 μ M, they become nearly indiscernible. At the higher phenylacrylate concentrations, it is evident that the system does not reach a steady state even after 5 s as the absorbance continues to change; this is most noticeable at 1 mM phenylacrylate (Figure 4A,B). However, at these higher concentrations and longer timescales, the absorbance changes are associated with multiple turnovers. As such, they reflect the approach of the system to chemical

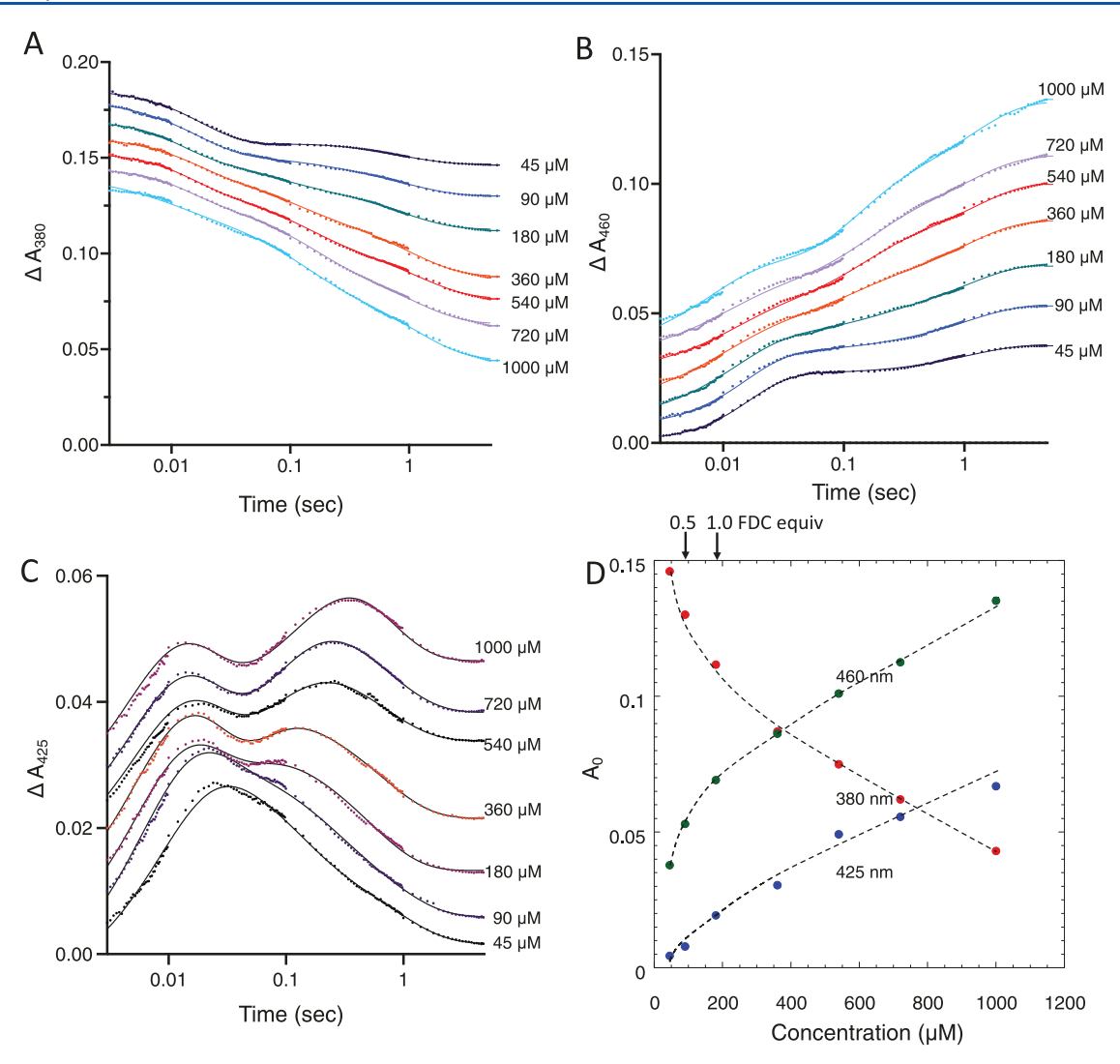


Figure 4. Pre-steady-state kinetics of FDC reacting with phenylacrylate. FDC was reacted with increasing concentrations of phenylacrylate as indicated, and the reaction was monitored at (A) 380 nm, (B) 460 nm, and (C) 425 nm. The data are shown with traces individually fitted to a four-exponential function; however, as discussed in the text, it was not possible to obtain robust values for individual rate constants from the fits. *Note:* the absorbance traces have been offset for clarity. (D) Total changes the absorbance (recorded after 5 s) at the different wavelengths are plotted as a function of styrene concentration for each wavelength monitored. The dashed lines are interpolated between the data points. The concentrations of styrene corresponding to 0.5 and 1.0 FDC active sites are marked above the plot.

equilibrium rather than reporting on the kinetics of chemical steps in the enzyme mechanism.

The complexity of the kinetic behavior observed with phenylacrylate, which required four apparent first-order rate constants to adequately model the data, meant that it was not possible to obtain robust fits to the data. As shown in Figure 4, all the traces could be reasonably well fitted using fourexponential functions, with residuals of $r^2 > 0.995$. But attempts to fit either individual traces, or globally fit the data, using Prism software to obtain values for the four rate constants resulted in values with either very wide or indeterminate confidence intervals (for details, see the Supporting Information). Nevertheless, the approximate values for the observed rate constants could be estimated from the data as $k_{1\text{phe}} \sim 150-200 \text{ s}^{-1}$, $k_{2\text{phe}} \sim 100 \text{ s}^{-1}$, $k_{3\text{phe}} \sim 8 \text{ s}^{-1}$, and $k_{\rm 4phe} \sim 1~{\rm s}^{-1}$. The values for $k_{\rm 1phe}$ and $k_{\rm 2phe}$ were subject to the greatest variation in trials to fit the data, whereas the values obtained for k_{3phe} and k_{4phe} were less dependent on the initial parameters used in fitting.

The initial reaction of prFMN with phenylacrylate, $k_{\rm 1phe} \sim 150-200~{\rm s}^{-1}$, occurs significantly faster than that of styrene, $k_{\rm 1sty} = 42~{\rm s}^{-1}$, which may reflect the higher intrinsic reactivity of phenylacrylate toward dipolar cycloaddition. The second phase of the reaction is also rapid, $k_{\rm 2phe} \sim 100~{\rm s}^{-1}$; we tentatively assign this phase to the decarboxylation of the prFMN-phenylacrylate cycloadduct to form the prFMN-styrene cycloadduct, which previous work has shown is the adduct that accumulates on the enzyme. As discussed below, we propose that $k_{\rm 3phe}$ is likely associated with product release. It is unclear what process gives rise to $k_{\rm 4phe}$, but in any case, this process is too slow for it to play a role in the catalytic cycle.

DISCUSSION

The prFMN-dependent class of decarboxylases catalyzes (de)carboxylation reactions at sp²-hybridized carbon atoms in an increasingly diverse range of substrates. These range from complex natural products to simple aromatic molecules. The enzymes so far characterized catalyze reactions on

aromatic rings,^{29,30} heterocyclic aromatic rings,^{25–28,31} and conjugated double bonds. Most intriguingly, indirect evidence suggests that prFMN-dependent enzymes may even catalyze the carboxylation of benzene to support the growth of some anaerobic bacteria.^{32,33} Although a number of enzymes have been structurally characterized,^{11,22,25,28,29,34} our understanding of the kinetics of prFMN-mediated catalysis remains poorly developed. A deeper understanding of prFMN reactivity is an important prerequisite for effectively utilizing these enzymes for biocatalysis. Our studies have focused on defining the kinetic profile of FDC because it remains the best-characterized member of the prFMN-dependent decarboxylase family and the chemical steps in the mechanism are most clearly defined.

Here, we have investigated the pre-steady-state kinetics of FDC reacting with phenylacrylate and styrene over concentrations that range from sub-stochiometric to a several-fold molar excess with respect to enzyme active sites. The kinetics of both reactions are surprisingly complicated, and this complexity precludes an unambiguous interpretation of all the kinetic features. Nevertheless, we consider that the concentration-dependence of the reaction kinetics may reasonably be explained by invoking negative cooperativity (half-of-the-sites reactivity) between the active sites of the FDC dimer.

The reaction with styrene provides the clearest evidence for negative cooperativity because it can only form the prFMN–styrene cycloadduct and does not react further (proton abstraction from the cycloadduct occurs orders of magnitude more slowly). Here, although only single chemical reaction can occur, three apparent first-order rate constants are needed to adequately fit the data. The concentration-dependence of the kinetic data clearly suggests that the two active sites have different affinities for styrene. The fastest phase of the reaction, characterized by $k_{1\text{sty}} = 45 \text{ s}^{-1}$, dominates at low substrate concentrations; however, once the styrene:enzyme ratio exceeds 0.5, the slower phase of the reaction, characterized by $k_{2\text{sty}} = 8.2 \text{ s}^{-1}$, starts to increase in amplitude and becomes prominent (Figure 3D).

A similar pattern of concentration-dependent kinetic behavior is seen in the reaction of phenylacrylate. In this case, the two fastest phases of the reaction, characterized by $k_{\rm 1phe}\sim150-200~{\rm s}^{-1}$ and $k_{\rm 2phe}\sim100~{\rm s}^{-1}$, are prominent at low substrate concentrations. We attribute these to the initial formation of the phenylacrylate–prFMN cycloadduct and its conversion to the styrene–prFMN cycloadduct at the "fast-tight" site. Only after the phenylacrylate:enzyme ratio exceeds 0.5 does the slower phase characterized by $k_{\rm 3phe}\sim8~{\rm s}^{-1}$ gain in amplitude (Figure 4D). Although the assignment of the various apparent rate constants to chemical processes remains somewhat tentative, this type of concentration-dependent kinetic behavior is a hallmark of half-of-the-sites reactivity.

Crystal structures are now available for a number of UbiD-like enzymes (recently reviewed in ref 36) that show different enzymes to adopt dimeric, tetrameric, or hexameric structures. However, these structures do not provide any obvious evidence for negative cooperativity, for example, by revealing asymmetry between the protein subunits. Nevertheless, it appears that domain movements are likely to be important for substrate binding and catalysis such movements have been captured in the open and closed structures of vanillic acid decarboxylase.³⁷ Similar domain-scale motions have not been documented for FDC, but smaller-scale active site motions

have been observed in structures of FDC complexed with various mechanism-based inhibitors that mimic intermediates in the reaction.²² Although the various structures of FDC fail to provide evidence for cooperativity, we note that the transient and often subtle motions involved in allosteric interactions are hard to capture by crystallography.

The question that arises is does this putative negative cooperativity have any mechanistic significance? We argue that it may play a role in facilitating the release of styrene from FDC. We note that even at the lowest concentration of phenylacrylate used in these experiments (45 μ M), the enzyme does not return to the resting state. Even after 5 s, we see no evidence for styrene dissociating from the active site, which would show up as an increase in absorbance at 380 nm or a decrease at 460 nm as prFMN is regenerated. This observation implies that styrene remains tightly bound to the enzyme as its prFMN cycloadduct rather than undergoing cycloelimination to complete turnover. Thus, the "fast, tight" site does not appear to be kinetically competent to perform the *complete* reaction cycle.

One explanation is that FDC is severely product-inhibited by styrene, and because these experiments require relatively high concentrations of the enzyme (180 μ M), the accumulation of styrene—prFMN adducts is favored, whereas lower concentrations would allow styrene to diffuse from the enzyme. We consider this explanation unlikely because the $K_{\rm M}$ for phenylacrylate is 180 μ M, ²³ implying that the enzyme would become product-inhibited at substrate concentrations well below $K_{\rm M}$. Also, there are no enzymes known in yeast that further metabolize styrene to prevent its build-up in the cell—it is assumed to be removed by diffusion. Rather, we propose that negative cooperativity plays a key role in the catalytic cycle of FDC by providing a mechanism that ejects styrene from the enzyme after decarboxylation.

In this mechanism, outlined in Figure 5, the substrate initially binds and undergoes decarboxylation rapidly at the "fast, tight" active site. Next, at higher substrate concentrations, the substrate will bind to the "slow, loose" active site. The effect of substrate binding at the second active site will be to push the low-affinity site toward the high-affinity state, resulting in a protein conformational change that flips the "fast, tight" site to the "slow, loose" state and vice versa. This conformational change now places styrene in the low-affinity active site, causing it to undergo cycloelimination to complete the first catalytic cycle. Phenylacrylate is now in the highaffinity active site, where it undergoes cycloaddition and decarboxylation to styrene. Thus, catalysis proceeds through rounds of substrate binding at one site and product release at the other that drives an alternating "two-stroke" catalytic cycle. This cycling provides a mechanism in which the energetically favorable cycloaddition and decarboxylation steps occurring at one active site are coupled to the unfavorable cycloelimination of styrene at the other active site.

In support of this mechanism, our measurements with higher concentrations of substrate show that the low-affinity active site reacts with phenylacrylate to form the prFMN—phenylacrylate cycloadduct with $k_{\rm 3phe}\sim 8~{\rm s}^{-1}$, which is very similar both to the rate at which styrene reacts at the second site, $k_{\rm 2sty}=8.2~{\rm s}^{-1}$, and to $k_{\rm cat}=7~{\rm s}^{-1}$ determined from steady-state kinetic analysis. In addition, various lines of evidence point to styrene release being rate-limiting in the reaction and therefore the step that primarily determines $k_{\rm cat}$. These include the observation by mass spectrometry of stable prFMN—

Biochemistry pubs.acs.org/biochemistry Article

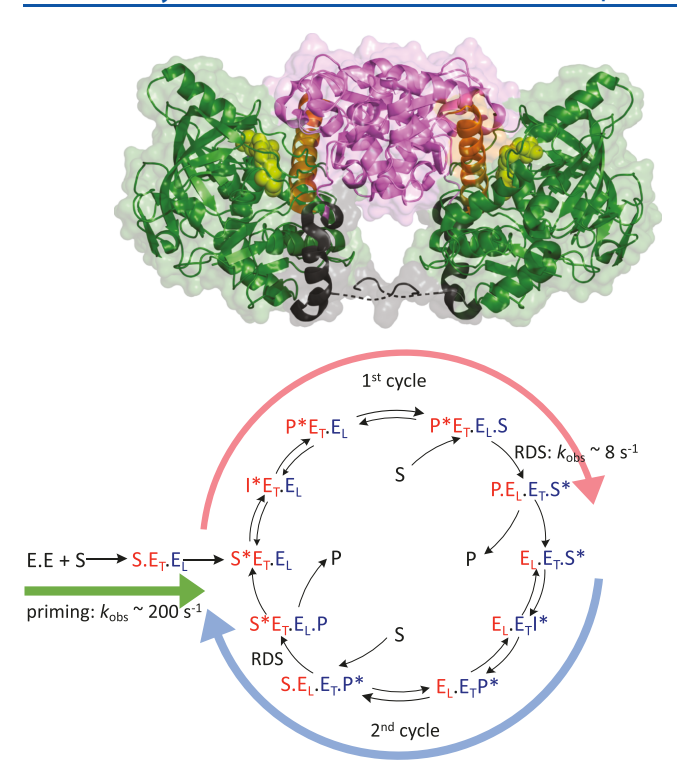


Figure 5. Proposed catalytic cycle for FDC-catalyzed decarboxylation incorporating negative cooperativity. Top: The structure of the FDC dimer highlighting the domain organization (PDB: 4ZA4). The dimerization and catalytic domains are colored magenta and green, respectively; the domain-connecting helix is shown in orange and the C-terminal helix in black. prFMN is colored yellow. Bottom: The proposed "two-stroke" mechanism for decarboxylation. The priming phase involves the initial substrate-binding event that differentiates the two active sites, color-coded red and blue, into a tight-binding (E_T) and loose-binding (E_L) site. In the first cycle, the substrate reacts with prFMN at the "red" active site; S*, I*, and P* represent covalent adducts C, D, and E in Figure 1. Reaction of the substrate at the "blue" active site results in interconversion of the "T" and "L" forms of the enzyme resulting cycloelimination of P in the rate-determining step (RDS). The second cycle proceeds analogously through reaction at the "blue" active site.

styrene cycloadducts formed in the FDC reaction; ²³ the large, normal 2°KIE = 1.15 ± 0.017 measured on $V_{\rm max}/K_{\rm M}$ under steady-state conditions for the decarboxylation of d₇-phenylacrylate; ³⁸ and the negative ρ value for the reaction determined from Hammett analysis of the enzyme reported previously. ³⁸

We note that some aspects of the kinetics remain puzzling. Particularly unusual is the apparent lack of concentration dependence on the rates of reaction for the various phases. The concentration dependence of the amplitudes associated with $k_{3\text{phe}}$ and $k_{2\text{sty}}$ indicates that the "slow, loose" active site does not become saturated with the substrate under the conditions of the experiment. (The maximum concentration of styrene in the experiment is limited by its solubility in water.) However, such behavior would normally be accompanied by a marked concentration dependence on the rate of reaction as well. This suggests that a kinetic step that is independent of substrate binding is rate-limiting for this step of the reaction. This type of kinetic behavior might arise from a "gating" motion of the protein, and indeed, structural studies on several UbiD enzymes point to importance of protein motions in catalysis. Crucially though, any such motion would have to occur independently of substrate binding to explain the lack of concentration-dependence on the rate of reaction.

A further unusual feature of the kinetic behavior is the amplitudes of the absorbance changes associated with the "fast" and "slow" active sites are quite different. A priori one would expect that half-of-the-sites behavior would result in the amplitudes being of similar magnitude, but it is clear from the data in Figures 3 and 4 that the slower phases are associated with significantly larger absorbance changes. Again, it is currently unclear why this occurs. It is possible that the extinction coefficients associated with the two active sites may be different, and in this context, we note that the electronic spectra of flavins are very sensitive to the local environment of the protein. On the other hand, this behavior may reflect further kinetic complexity in which the internal equilibria coupling the various reaction species are different at each active site so that the prFMN adducts accumulate to different degrees.

We also note that prFMN has been observed in some FDC crystal structures with a hydroxyl group at C-1'. This inactive adduct is presumably in equilibrium with the active iminium form of prFMN. LC-MS analysis of holo-FDC used in our experiments provided no evidence for this adduct. However, the presence of such an equilibrium may additionally complicate kinetic analysis, especially if the equilibrium is perturbed by substrate binding.

These unusual features of the kinetics, together with the complexity of the kinetic traces, frustrated our attempts to fit the data to a kinetic model of the FDC reaction. Extensive attempts were made to evaluate various kinetic schemes, either incorporating or omitting cooperativity, using kinetic modeling software such as Kintek Explorer. However, simple kinetic models failed to provide convincing fits to the stopped-flow traces, whereas more complex models became over-parameterized and yielded either unrealistic and/or poorly constrained values for elementary rate constants.

CONCLUSIONS

Although an increasing number of prFMN-dependent enzymes are now known, and detailed structural information available for several of them, the kinetics of prFMN-catalyzed decarboxylation remains underdeveloped. Our experiments on FDC are the first to examine the pre-steady-state kinetics of a prFMN enzyme reacting with substrates under and single turnover conditions. These experiments reveal complex kinetic behavior that may be explained by negative cooperativity between the two active sites of the dimeric enzyme that results in a "fast, tight" site and a "slow, loose" site. We propose that interconversion between the "fast, tight" and "slow, loose" sites may play an important role in the mechanism by driving the release of styrene from the enzyme, which is the ratedetermining step of the overall reaction. We note that all UbiD enzymes so far characterized possess dimeric, tetrameric, or hexameric quaternary structures, with the dimer forming the basic functional unit. It is therefore possible that a similar "twostroke" kinetic mechanism may be a general feature of the decarboxylation reactions catalyzed by this class of enzymes.

A necessary caveat to these conclusions is that the complexity of the kinetics still leaves several features of the reaction unexplained. This leaves open the possibility that mechanisms other than negative cooperativity are responsible for the multiphasic pre-steady-state kinetic behavior we observe. Additional experiments will be needed to allow the

reaction mechanism to be fully elucidated and a robust kinetic model developed.

ASSOCIATED CONTENT

Supporting Information

The Supporting Information is available free of charge at https://pubs.acs.org/doi/10.1021/acs.biochem.2c00460.

Tables summarizing rate constants obtained from fitting the kinetic data presented in the paper (PDF)

AUTHOR INFORMATION

Corresponding Author

E. Neil G. Marsh – Department of Chemistry and Department of Biological Chemistry, University of Michigan, Ann Arbor, Michigan 48109, United States; orcid.org/0000-0003-1713-1683; Email: nmarsh@umich.edu

Authors

April K. Kaneshiro – Department of Chemistry and Department of Biological Chemistry, University of Michigan, Ann Arbor, Michigan 48109, United States

Prathamesh M. Datar — Department of Chemistry, University of Michigan, Ann Arbor, Michigan 48109, United States; orcid.org/0000-0003-1514-9767

Complete contact information is available at: https://pubs.acs.org/10.1021/acs.biochem.2c00460

Author Contributions

All the authors contributed in preparing the manuscript. A.K.K. conducted the experiments and analyzed the data. P.M.D. analyzed the kinetic data. A.K.K., P.M.D., and E.N.G.M. wrote the manuscript. E.N.G.M. conceptualized the idea for the manuscript.

Funding

This research was supported by the National Science Foundation grants CHE 1608553 and CHE 1904759 to E.N.G.M.

Notes

The authors declare no competing financial interest. Ferulic acid decarboxylase 1 Q03034.

ACKNOWLEDGMENTS

The authors thank Dr. Bruce Palfey for assistance in acquiring the stopped-flow data and valuable discussions on its analysis and interpretation.

ABBREVIATIONS USED

FDC, ferulic acid decarboxylase; prFMN, prenylated-flavin mononucleotide

REFERENCES

- (1) Miller, B. G.; Wolfenden, R. Catalytic Proficiency: The Unusual Case of OMP Decarboxylase. *Ann. Rev. Biochem.* **2002**, *71*, 847–885.
- (2) Wolfenden, R. Benchmark Reaction Rates, the Stability of Biological Molecules in Water, and the Evolution of Catalytic Power in Enzymes. *Ann. Rev. Biochem.* **2011**, *80*, 645–667.
- (3) Belcher, J.; McLean, K. J.; Matthews, S.; Woodward, L. S.; Fisher, K.; Rigby, S. E. J.; Nelson, D. R.; Potts, D.; Baynham, M. T.; Parker, D. A.; Leys, D.; Munro, A. W. Structure and Biochemical Properties of the Alkene Producing Cytochrome P450 OleTJE (CYP152L1) from the Jeotgalicoccus sp. 8456 Bacterium. *J. Biol. Chem.* 2014, 289, 6535–6550.

- (4) Cleland, W. W. Mechanisms of Enzymatic Oxidative Decarboxylation. Acc. Chem.Res. 1999, 32, 862-868.
- (5) Jordan, F.; Patel, H. Catalysis in Enzymatic Decarboxylations: Comparison of Selected Cofactor-Dependent and Cofactor-Independent Examples. *ACS Catal.* **2013**, *3*, 1601–1617.
- (6) Keasling, J. D. Manufacturing Molecules Through Metabolic Engineering. *Science* **2010**, *330*, 1355–1358.
- (7) Kourist, R.; Guterl, J.-K.; Miyamoto, K.; Sieber, V. Enzymatic Decarboxylation-An Emerging Reaction for Chemicals Production from Renewable Resources. *ChemCatChem* **2014**, *6*, 689–701.
- (8) Leys, D. Flavin metamorphosis: cofactor transformation through prenylation. *Curr. Opin. Chem. Biol.* **2018**, *47*, 117–125.
- (9) Leys, D.; Scrutton, N. S. Sweating the assets of flavin cofactors: new insight of chemical versatility from knowledge of structure and mechanism. *Curr. Opin. Struct. Biol.* **2016**, *41*, 19–26.
- (10) Lin, F.; Ferguson, K. L.; Boyer, D. R.; Lin, X. N.; Marsh, E. N. G. Isofunctional Enzymes PAD1 and UbiX Catalyze Formation of a Novel Cofactor Required by Ferulic Acid Decarboxylase and 4-Hydroxy-3-polyprenylbenzoic Acid Decarboxylase. *ACS Chem. Biol.* **2015**, *10*, 1137–1144.
- (11) Payne, K. A. P.; White, M. D.; Fisher, K.; Khara, B.; Bailey, S. S.; Parker, D.; Rattray, N. J. W.; Trivedi, D. K.; Goodacre, R.; Beveridge, R.; Barran, P.; Rigby, S. E. J.; Scrutton, N. S.; Hay, S.; Leys, D. New cofactor supports α,β -unsaturated acid decarboxylation via 1,3-dipolar cycloaddition. *Nature* **2015**, *522*, 497–501.
- (12) Piano, V.; Palfey, B. A.; Mattevi, A. Flavins as Covalent Catalysts: New Mechanisms Emerge. *Trends Biochem. Sci..* **2017**, 42, 457–469.
- (13) Wang, P.-H.; Khusnutdinova, A. N.; Luo, F.; Xiao, J.; Nemr, K.; Flick, R.; Brown, G.; Mahadevan, R.; Edwards, E. A.; Yakunin, A. F. Biosynthesis and Activity of Prenylated FMN Cofactors. *Cell Chem. Biol.* **2018**, 25, 560–570.e6.
- (14) Bloor, S.; Michurin, I.; Titchiner, G. R.; Leys, D. Prenylated flavins: structures and mechanisms *FEBS J.* 2022, DOI: 10.1111/febs.16371.
- (15) White, M. D.; Payne, K. A. P.; Fisher, K.; Marshall, S. A.; Parker, D.; Rattray, N. J. W.; Trivedi, D. K.; Goodacre, R.; Rigby, S. E. J.; Scrutton, N. S.; Hay, S.; Leys, D. UbiX is a flavin prenyltransferase required for bacterial ubiquinone biosynthesis. *Nature* **2015**, *522*, 502–506.
- (16) Arunrattanamook, N.; Marsh, E. N. G. Kinetic Characterization of Prenyl-Flavin Synthase from *Saccharomyces cerevisiae*. *Biochemistry* **2018**, *57*, 696–700.
- (17) Marshall, S. A.; Payne, K. A. P.; Fisher, K.; White, M. D.; A, N. C.; Balaikaite, A.; Rigby, S. E. J.; Leys, D. The UbiX flavin prenyltransferase reaction mechanism resembles class I terpene cyclase chemistry. *Nat. Commun.* **2019**, *10*, No. 2357.
- (18) Bentinger, M.; Tekle, M.; Dallner, G. Coenzyme Q Biosynthesis and functions. *Biochem. Biophys. Res. Comm.* **2010**, 396, 74–79.
- (19) Gulmezian, M.; Hyman, K. R.; Marbois, B. N.; Clarke, C. F.; Javor, G. T. The role of UbiX in Escherichia coli coenzyme Q biosynthesis. *Arch. Biochem. Biophys.* **2007**, *467*, 144–153.
- (20) Zhang, H.; Javor, G. T. Regulation of the isofunctional genes ubiD and ubiX of the ubiquinone biosynthetic pathway of Escherichia coli. *FEMS Microbiol. Lett.* **2003**, 223, 67–72.
- (21) Ferguson, K. L.; Eschweiler, J. D.; Ruotolo, B. T.; Marsh, E. N. G. Evidence for a 1,3-Dipolar Cyclo-addition Mechanism in the Decarboxylation of Phenylacrylic Acids Catalyzed by Ferulic Acid Decarboxylase. *J. Am. Chem. Soc.* **2017**, *139*, 10972–10975.
- (22) Bailey, S. S.; Payne, K. A. P.; Saaret, A.; Marshall, S. A.; Gostimskaya, I.; Kosov, I.; Fisher, K.; Hay, S.; Leys, D. Enzymatic control of cycloadduct conformation ensures reversible 1,3-dipolar cycloaddition in a prFMN-dependent decarboxylase. *Nat. Chem.* **2019**, *11*, 1049–1057.
- (23) Kaneshiro, A. K.; Koebke, K. J.; Zhao, C. Y.; Ferguson, K. L.; Ballou, D. P.; Palfey, B. A.; Ruotolo, B. T.; Marsh, E. N. G. Kinetic Analysis of Transient Intermediates in the Mechanism of Prenyl-

- Flavin-Dependent Ferulic Acid Decarboxylase. *Biochemistry* **2021**, *60*, 125–134.
- (24) Tian, G.; Liu, Y. Mechanistic insights into the catalytic reaction of ferulic acid decarboxylase from Aspergillus niger: a QM/MM study. *Phys. Chem. Phys.* **2017**, *19*, 7733–7742.
- (25) Payne, K. A. P.; Marshall, S. A.; Fisher, K.; Rigby, S. E. J.; Cliff, M. J.; Spiess, R.; Cannas, D. M.; Larrosa, I.; Hay, S.; Leys, D. Structure and Mechanism of Pseudomonas aeruginosa PA0254/HudA, a prFMN-Dependent Pyrrole-2-carboxylic Acid Decarboxylase Linked to Virulence. ACS Catal. 2021, 11, 2865–2878.
- (26) Kawanabe, K.; Aono, R.; Kino, K. 2,5-Furandicarboxylic acid production from furfural by sequential biocatalytic reactions. *J. Biosci. Bioeng.* **2021**, *132*, 18–24.
- (27) Datar, P. M.; Marsh, E. N. G. Decarboxylation of Aromatic Carboxylic Acids by the Prenylated-FMN-dependent Enzyme Phenazine-1-carboxylic Acid Decarboxylase. *ACS Catal.* **2021**, *11*, 11723–11732.
- (28) Payne, K. A. P.; Marshall, S. A.; Fisher, K.; Cliff, M. J.; Cannas, D. M.; Yan, C. Y.; Heyes, D. J.; Parker, D. A.; Larrosa, I.; Leys, D. Enzymatic Carboxylation of 2-Furoic Acid Yields 2,5-Furandicarboxylic Acid (FDCA). ACS Catal. 2019, 9, 2854–2865.
- (29) Payer, S. E.; Marshall, S. A.; Bärland, N.; Sheng, X.; Reiter, T.; Dordic, A.; Steinkellner, G.; Wuensch, C.; Kaltwasser, S.; Fisher, K.; Rigby, S. E. J.; Macheroux, P.; Vonck, J.; Gruber, K.; Faber, K.; Himo, F.; Leys, D.; Pavkov-Keller, T.; Glueck, S. M. Regioselective para-Carboxylation of Catechols with a Prenylated Flavin Dependent Decarboxylase. *Angew. Chem., Int. Ed.* **2017**, *56*, 13893–13897.
- (30) Boll, M.; Geiger, R.; Junghare, M.; Schink, B. Microbial degradation of phthalates: biochemistry and environmental implications. *Environ. Microbiol. Rep.* **2020**, *12*, 3–15.
- (31) Payer, S. E.; Faber, K.; Glueck, S. M. Non-Oxidative Enzymatic (De)Carboxylation of (Hetero)Aromatics and Acrylic Acid Derivatives. *Adv. Synth. Catal.* **2019**, *361*, 2402–2420.
- (32) Abu Laban, N.; Selesi, D.; Rattei, T.; Tischler, P.; Meckenstock, R. U. Identification of enzymes involved in anaerobic benzene degradation by a strictly anaerobic iron-reducing enrichment culture. *Environ. Microbiol.* **2010**, *12*, 2783–2796.
- (33) Meckenstock, R. U.; Boll, M.; Mouttaki, H.; Koelschbach, J. S.; Tarouco, P. C.; Weyrauch, P.; Dong, X. Y.; Himmelberg, A. M. Anaerobic Degradation of Benzene and Polycyclic Aromatic Hydrocarbons. *Microbiol. Physiol.* **2016**, *26*, 92–118.
- (34) Annaval, T.; Han, L.; Rudolf, J. D.; Xie, G. B.; Yang, D.; Chang, C. Y.; Ma, M.; Crnovcic, I.; Miller, M. D.; Soman, J.; Xu, W. J.; Phillips, G. N.; Shen, B. Biochemical and Structural Characterization of TtnD, a Prenylated FMN-Dependent Decarboxylase from the Tautomycetin Biosynthetic Pathway. ACS Chem. Biol. 2018, 13, 2728–2738.
- (35) Wielgus-Kutrowska, B.; Grycuk, T.; Bzowska, A. Part-of-thesites binding and reactivity in the homooligomeric enzymes facts and artifacts. *Arch. Biochem. Biophys.* **2018**, *642*, 31–45.
- (36) Roberts, G. W.; Leys, D. Structural insights into UbiD reversible decarboxylation. *Curr. Opin. Struct. Biol.* **2022**, *75*, 102432.
- (37) Marshall, S. A.; Payne, K. A. P.; Fisher, K.; Titchiner, G. R.; Levy, C.; Hay, S.; Leys, D. UbiD domain dynamics underpins aromatic decarboxylation. *Nat. Commun.* **2021**, *12*, No. 5065.
- (38) Ferguson, K. L.; Arunrattanamook, N.; Marsh, E. N. G. Mechanism of the Novel Prenylated Flavin-Containing Enzyme Ferulic Acid Decarboxylase Probed by Isotope Effects and Linear Free-Energy Relationships. *Biochemistry* **2016**, *55*, 2857–2863.